

NANO MICRO
small

Supporting Information

for *Small*, DOI: 10.1002/smll.201501883

Photo-electrochemical Bioanalysis of Guanosine
Monophosphate Using Coupled Enzymatic Reactions at a
CdS/ZnS Quantum Dot Electrode

*Nadeem Sabir, Nazimuddin Khan, Johannes Völkner, Felix
Widdascheck, Pablo del Pino, Gregor Witte, Marc Riedel,
Fred Lisdat,* Manfred Konrad,* and Wolfgang J. Parak**

Photoelectrochemical bioanalysis of guanosine monophosphate via the use of coupled enzymatic reactions at a CdS/ZnS quantum dot electrode

Nadeem Sabir^{1§}, Nazimuddin Khan^{2§}, Johannes Völkner¹, Felix Widdascheck¹, Pablo del Pino³, Gregor Witte¹, Marc Riedel⁴, Fred Lisdat^{4*}, Manfred Konrad^{2*}, Wolfgang J. Parak^{1,3*}

¹ Fachbereich Physik, Philipps Universität Marburg, Marburg, Germany

² Max Planck Institute for Biophysical Chemistry, Göttingen, Germany

³ CIC biomaGUNE, San Sebastian, Spain

⁴ Biosystems Technology, Institute of Applied Life Sciences, Technical University Wildau, Wildau, Germany

* corresponding authors: flisdat@th-wildau.de, mkonrad@mpibpc.mpg.de,
wolfgang.parak@physik.uni-marburg.de

§ contributed equally

Supporting Information

I) Materials and Methods

I.1) Reagents

I.2) Quantum dot synthesis

I.3) Preparation of the Au electrode and immobilization of dithiol on Au

I.4) Electrochemical cell and measurement set-up

II) Measurements

II.1) Photocurrent measurements of the QD electrode following the pyruvate conversion (third reaction)

II.2) Photocurrent measurements of the QD electrode with the reactants of the first enzyme reaction

II.3) Photocurrent measurements of the QD electrode in solutions with the reactants of the first and second enzyme reaction

II.4) Photocurrent measurements of the QD electrode with all the three enzymes in solution

II.5) Photocurrent measurements of the QD sensor electrode immobilized enzymes

III) References

I) Materials and Methods

I.1) Reagents

Cadmium oxide (99.99%), sulfur powder (99.99%), trioctylphosphine oxide (TOPO, 99%), hexadecylamine (HDA, technical grade 90%), diethyl zinc solution ($C_4H_{10}Zn$, 1.0 M solution in heptane), hexamethyldisilathiane ($C_6H_{18}Si_2S$), 1-octadecene (ODE, technical grade 90%), oleylamine (OA, technical grade 70%), poly(sodium 4-styrenesulfonate) (PSS, $M_w \approx 70$ kDa, #243051) and poly(allylamine hydrochloride) (PAH, $M_w \approx 56$ kDa, #283223), Adenosine 5'-triphosphate (ATP), guanosine-5'-monophosphate (GMP), pyruvic acid, pyruvate kinase (PK), lactate dehydrogenase (LDH), and 4,4'-dimercaptostilbene (StDT, >96%) were purchased from Sigma-Aldrich; zinc stearate (count as $ZnO\% \approx 14\%$) from Alfa Aesar; tri-n-butylphosphine (TBP, 99%) from ABCR GmbH & Co. KG; $MgCl_2$ and KCl from Merck (Darmstadt, Germany); methanol, acetone, toluene, hexane and HEPES from Carl Roth GmbH + Co. KG (Karlsruhe, Germany); nicotinamide adenine dinucleotide reduced (NADH) and phosphoenolpyruvate (PEP) from Roche Diagnostic GmbH (Mannheim, Germany). Human guanylate kinase (GMPK) was expressed and purified as highly pure recombinant fusion protein with His₆-SUMO tag^[1].

I.2) Quantum dot synthesis

Synthesis of CdS nanoparticle (NP) cores, *i.e.* quantum dots (QDs), was carried out by using the procedure reported by Yu and Chen.^[2,3] Briefly, cadmium oxide (0.126 g), oleic acid (2.02 g), and ODE (12.0 mL) were added in a three-neck flask. The system was heated to 300 °C under nitrogen atmosphere after degassing. At this temperature, sulfur dissolved in ODE (0.25 M, 2.0 mL) was swiftly injected into the mixture. After the injection, the temperature was reduced to 240 °C for 3.5 minutes. For the precipitation of the QDs, toluene (10 mL) was added followed by 20-30 mL of acetone. The resulting solution was then centrifuged at 2000 rounds per minute (rpm) for 5 minutes, and the precipitate was re-dispersed in toluene. One more washing step was performed by adding 20-30 mL of methanol. The precipitate (after discarding of the supernatant) containing the CdS NPs was re-dispersed in hexane.

Growth of a ZnS shell on top of the CdS cores. A previously described protocol was used for the growth of a ZnS shell onto the CdS QDs.^[4] For this purpose, 4 g of TOPO and 1 g of HDA were weighed in a 50 mL 3-necked flask. The temperature of this mixture was increased under vacuum up to 120 °C for 20 minutes under stirring. After switching the vacuum to argon flow, an appropriate amount of CdS QD solution (NP concentration *ca* $c_{NP} = 4 \mu M$, NP concentrations were determined by UV/Vis absorption spectra according to Yu *et al.*^[5]) was injected into the TOPO/HDA mixture, and the chloroform was then removed under vacuum. After switching the vacuum to nitrogen, the temperature was raised to 170 °C according to published procedures^[6]. A stock solution for the ZnS shell growth was prepared by dissolving 0.31 g of diethylzinc solution and 0.45 g of hexamethyldisilathiane in 20.0 g TBP. The stock solution was added dropwise to the CdS/TOPO/HAD mixture. The amount of added stock

solution for growing the ZnS shell was calculated according to a previously published protocol.^[6] After adding the ZnS precursor, the temperature was reduced to 100 °C, and the solution was kept stirring for 2 hours. Then the reaction was stopped by removing the heating mantle, and the CdS/ZnS NPs were precipitated by adding methanol. After discarding of the supernatant, the NPs were re-dispersed in toluene. UV/Vis absorption and fluorescence spectra, as well as transmission electron microscopy (TEM) images of the resulting CdS/ZnS QDs are shown in Figure SI-I.2.1.

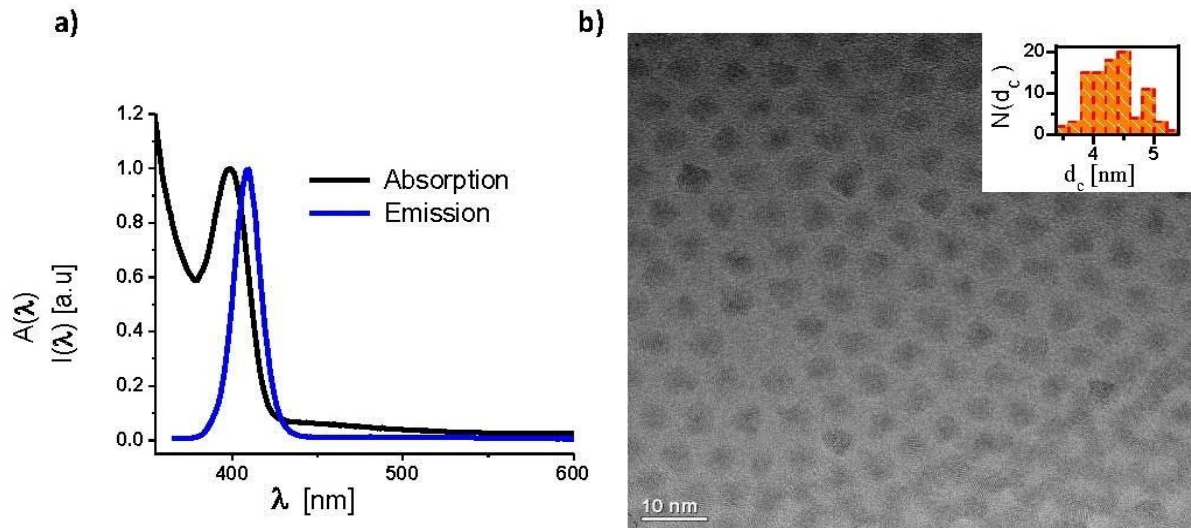


Figure SI-I.2.1: a) Normalized absorption $A(\lambda)$ (black line) and fluorescence $I(\lambda)$ spectra (blue line, emission at 409 nm) of CdS/ZnS QDs dissolved in toluene. The wavelengths of the first excitation peak in the absorption spectrum and of the maximum of the fluorescence emission of the CdS/ZnS NPs are $\lambda = 399$ nm and $\lambda = 409$ nm, respectively. The wavelengths of the first excitation peak in the absorption spectrum and of the maximum of the fluorescence emission of the underlying, original CdS NPs were $\lambda = 390$ nm and $\lambda = 398$ nm, respectively. b) TEM image of the CdS/ZnS QDs. The scale bar corresponds to 10 nm. The mean core diameter d_c of the CdS/ZnS NPs as determined from the size distribution $N(d_c)$ is $d_c = 4.4 \pm 0.4$ nm.

1.3) Preparation of the Au electrode and immobilization of dithiol on Au

Polished silicon wafers covered with a native oxide layer (SilchemHgbmh) were cut into pieces of 1 cm², rinsed with 2-propanol and ethanol and subsequently dried in a nitrogen stream. Gold was deposited *via* sputter deposition in argon plasma yielding a homogeneous film with a thickness of about 15 nm (Au/SiO₂).

Self-assembling monolayers (SAMs) of stilbenedithiol were prepared following previously established protocol.^[7] Au/SiO₂ substrates were immersed in a 100 nM solution of StDT in toluene for 24 hours at 75 °C, followed by subsequent rinsing with toluene and drying in a nitrogen stream to remove excess molecules. For daily experiments, individual solutions were prepared from a 100 μM stock solution in toluene which was renewed every month and stored refrigerated in the dark to avoid aging.

Please note that in this study instead of a massive Au electrode a thin Au film deposited on a Si chip was used as working electrode (Au/Si substrate). While for linking off the StDT layer to the surface of the working electrode the underlying Si substrate does not play a role, it may well influence details of signal generation. As Si is a semiconductor, electron-hole pairs may be also generated in the Si chip upon illumination, which can contribute to the photocurrent. In this way the underlying Si chip may be involved in the photocurrent in addition to the photocurrent originating from the QDs. However, the detailed source of the basic photocurrent is not of importance for the here described sensor assay.

I.4) Electrochemical cell and measurement set-up

The electrochemical measurement set-up consisted of five main parts: A light source, a chopper, an electrochemical cell, a three-electrode system, and a lock-in amplifier. This set up was described in previously published protocols.^[7-9]

Light Source: A Xe arc lamp (emission spectrum $\lambda_{em} = 300 - 700$ nm), controlled by a lamp power supply (LPS 220 by Photon Technology International), was used as a light source. The light from the arc lamp to the electrochemical cell was focused through a convex and a plano-convex lens coupled to a 45° mirror, as shown in the schematic diagram Figure SI-I.4.3. All the optical parts were purchased from Linos Germany. The illumination power (P_{illum}) of the resulting light spot of approximately 6 mm diameter was measured with a photometer (Fieldmaster photometer, Coherent). An illumination power of $P_{illum} = 23$ mW was used for electrochemical measurements reported in this work.

Optical chopper: An optical chopper (Scitec instruments) was used in the light prior to the convex lens to modulate the incident light at a desired frequency.

Electrochemical measurement cell: The electrochemical measurement cell harboring the Au chips is shown in Figure SI-I.4.3. It comprised a rectangular container which contained the buffer solution of up to 2 mL, and built a support for both, the reference and the counter electrode. Light entered the chamber from the top to hit the gold electrode on the bottom. At the bottom, the rectangular container contained a small hole of 6 mm diameter. The electrochemical cell was tightly sealed with screws as shown in Figure SI-I.4.1.

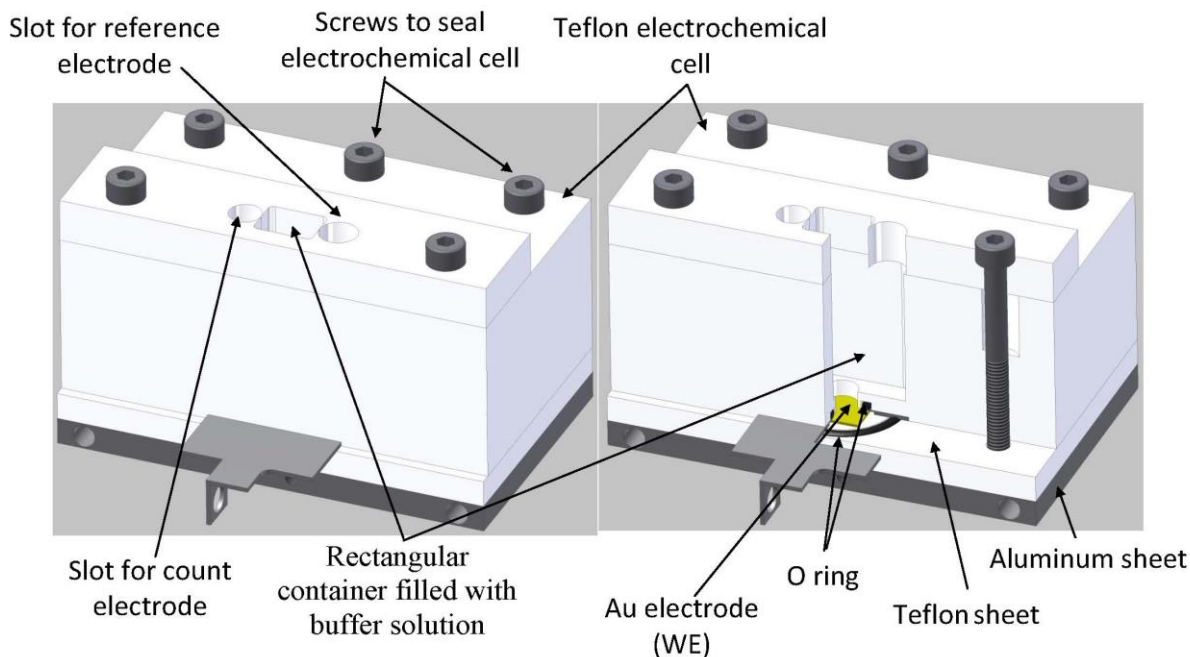


Figure SI-I.4.1: a) Complete view of the electrochemical cell showing the arrangement of the counter and reference electrode. b) Intersection view of the electrochemical cell. The Au electrode (working electrode) lies on the gold plated holder which is squeezed between the Teflon rectangular container and Teflon sheet with the help of an O-ring.

Three-electrode system: The important components of the three-electrode system were three electrodes and a microcomputer with an interface card for digital-to-analog (DAC) and analog-to-digital (ADC) conversion. An Ag/AgCl-saturated reference electrode (RE), a spiral wire of platinum as counter electrode (CE), and a gold chip as working electrode (WE) were assembled within the electrochemical cell as shown in Figure SI-I.4.3. The operational amplifiers OP1, OP2, and OP3 were mounted within the three-electrode arrangement as shown in Figure SI-I.4.2. The voltage U_{Ext} was applied by the DAC at the positive input of OP1 through OP3. The operational amplifier OP3 acted as an inverter and gave stable input. The RE was connected with the negative input of OP1. The resultant current I_{OP1} is zero, according to the characteristics of an OP (all input currents = 0), and thus no current flows through the RE. The potential difference between the RE and WE remains constant. To adjust the sensitivity of the instrument, a variable resistor was R_2 introduced in the circuit around OP2 between the negative input and the output of the OP2. This setup is called current-to-voltage converter. The output U_{out} of OP2 was measured by a lock-in amplifier followed by the ADC.

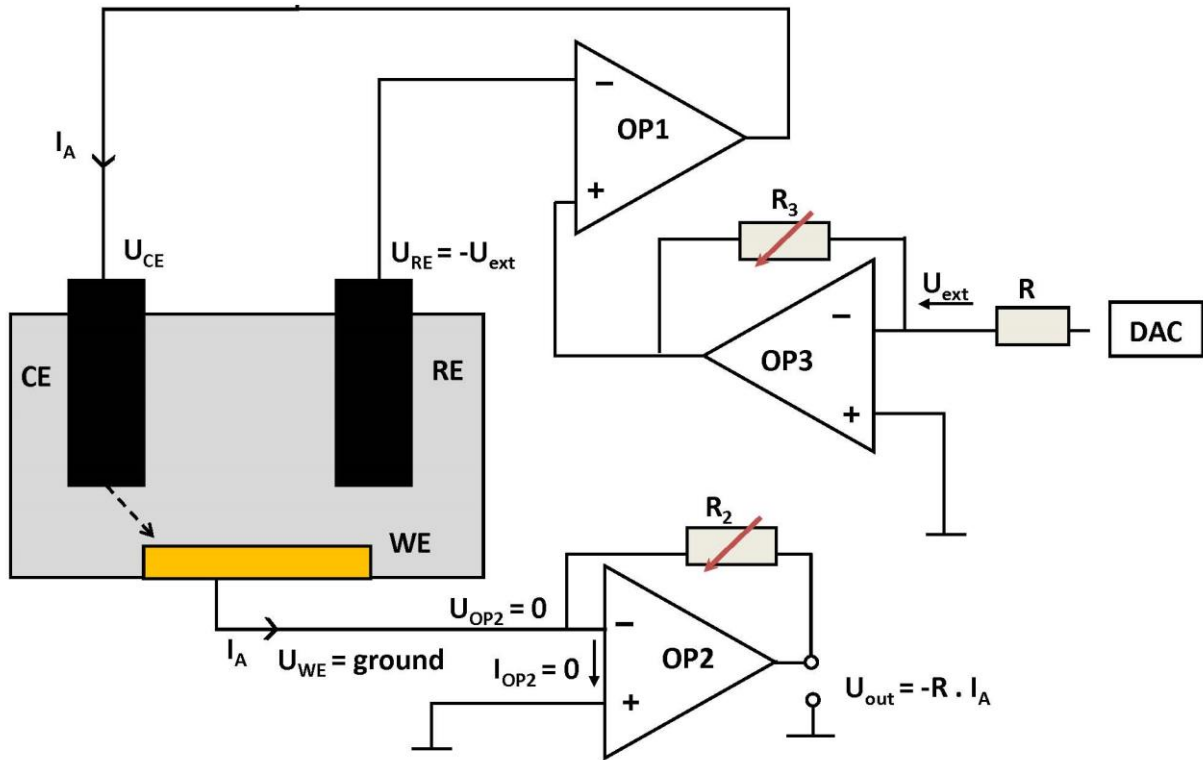


Figure SI-I.4.2: Schematics of a three-electrode system.

Lock-in amplifier: A lock-in amplifier (EG&G, Model # 5210) was used to improve the signal-to-noise ratio.^[9] A modulation frequency of 17.3 Hz for the chopper was used as a reference frequency for the lock-in. The lock-in amplifier filtered out all additional frequencies and amplified only the part of the input signal at the reference frequency. Throughout the experiment, for all the measurements, a time constant of 30 ms was used. The output of the lock-in amplifier was read by a serial port interface (DAC).

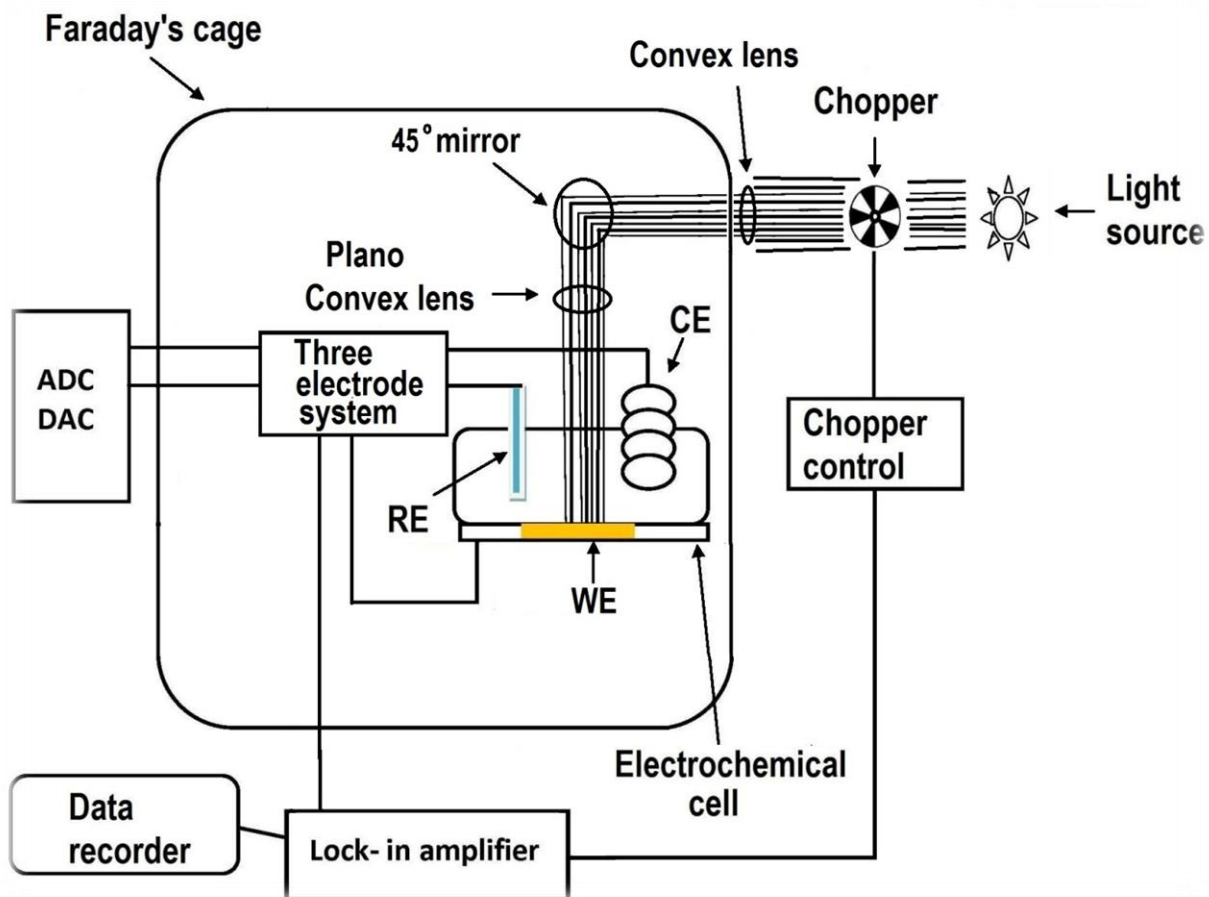


Figure SI-I.4.3: Schematic diagram of the set-up of the electronics to connect the electrochemical cell.

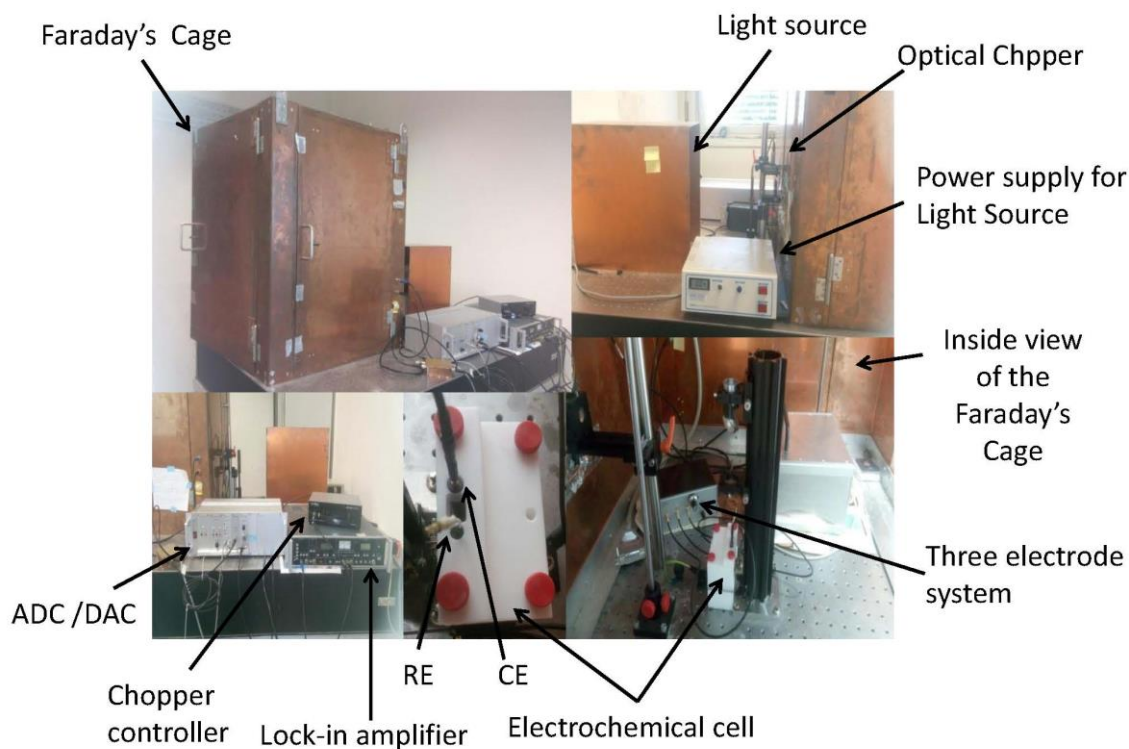


Figure SI-I.4.4: Photographs of the set-up.

II) Measurements

II.1) Photocurrent measurements of the QD electrode following the pyruvate conversion (third reaction)

The reaction according to Eq. 3 in the main text is sketched in Figure SI-II.1.1. Photocurrent measurements $I(t)$ in the presence of NADH, with and without LDH, and variable pyruvate concentrations, are shown in Figure SI-II.1.2. The modulated light was switched on and off in cycles of 30 s, and photocurrent only flew upon illumination. The concentration dependence is shown in Figure 2 of the paper. Enzymes (here LDH) were free in solution.

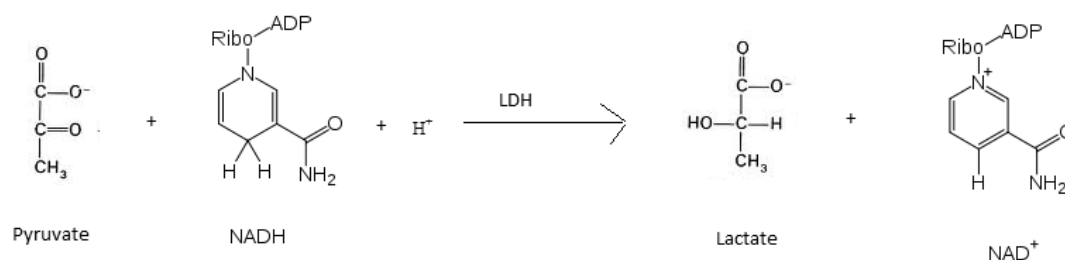


Figure SI-II.1.1: Schematic of the 3rd reaction catalyzed by lactate dehydrogenase.

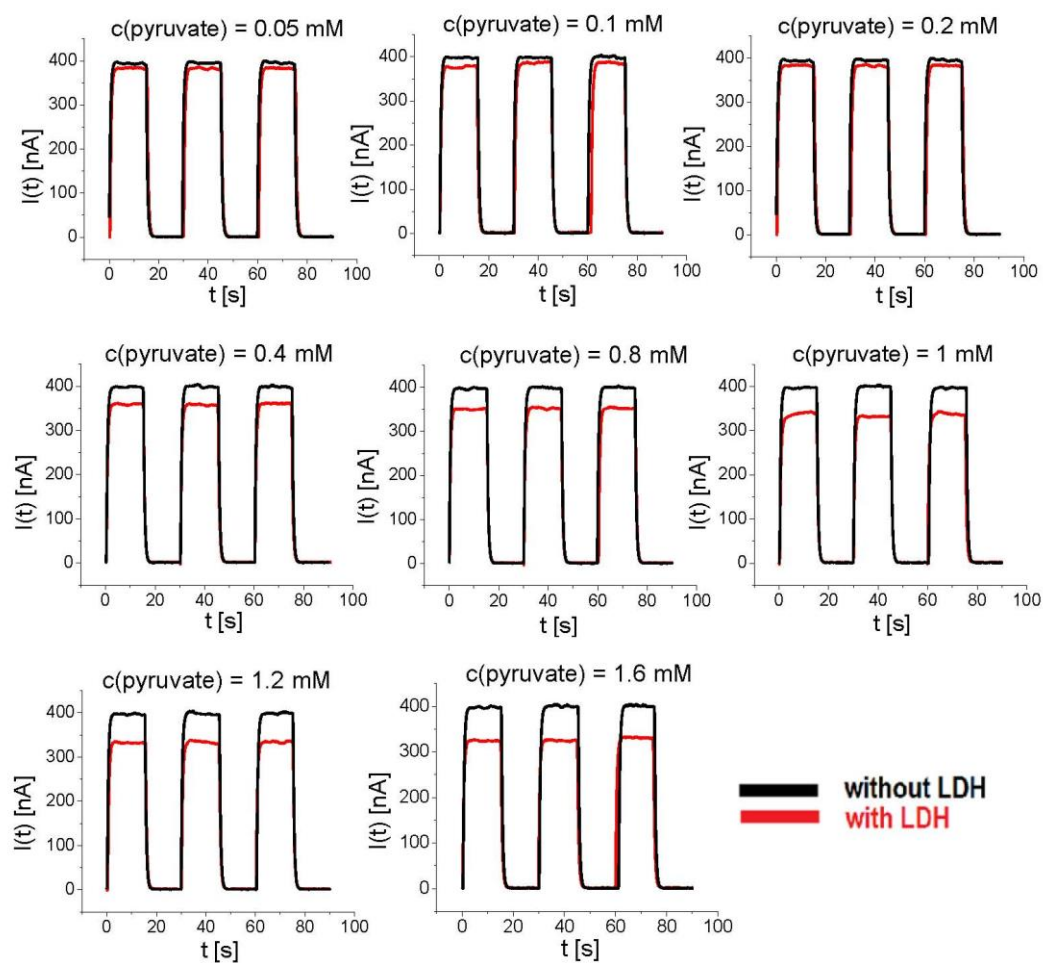


Figure SI-II.1.2: Photocurrent measurements $I(t)$ following the reaction of Eq. 3 with the following conditions: 1.2 mM NADH, 100 mM HEPES pH 7.5, 100 mM KCl, 20 mM MgCl₂,

$U_{bias} = +50 \text{ mV}$, $T = 25 \text{ }^\circ\text{C}$. LDH was optionally added (15 units/mL). Pyruvate concentrations $c(\text{pyruvate})$ were varied from 0.05 mM to 1.6 mM. The resulting amplitudes of the photocurrent versus the pyruvate concentration $I_{max}(c(\text{pyruvate}))$ are displayed in Figure SI-II.1.3. In Figure 2 of the main text, the amplitude of the photocurrent I_{max} versus the pyruvate concentration $c(\text{pyruvate})$ is plotted as the difference in photocurrent amplitude with (“w LDH”) and without LDH (“wo LDH”): $\Delta I_{max}(c(\text{pyruvate})) = I_{max}^{wLDH}(c(\text{pyruvate})) - I_{max}^{woLDH}(c(\text{pyruvate}))$.

Photocurrent measurements $I(t)$ for the reaction given in Eq. 3 and Figure SI-II.1.1 were also carried out for different bias voltages U_{bias} , cf. Figure SI-II.1.3 and Figure SI-II.1.4. U_{bias} is the applied voltage of the working electrode versus a homemade Ag/AgCl electrode. As in the investigated range there was no significant dependence from U_{bias} , in all following measurements U_{bias} was fixed to $U_{bias} = +50 \text{ mV}$.

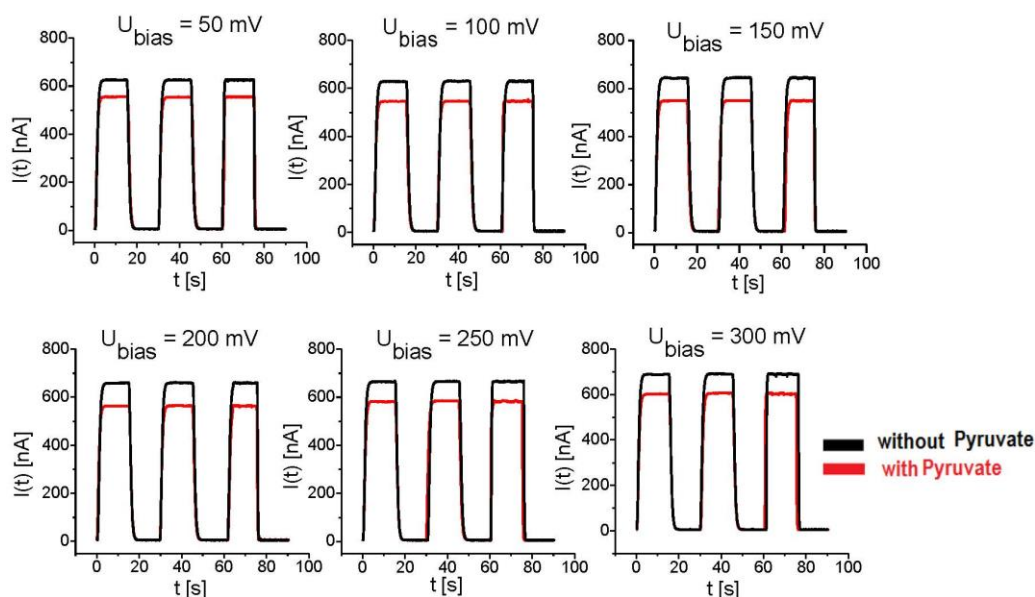


Figure SI-II.1.3: Photocurrent measurements $I(t)$ following the reaction of Eq. 3 with the following conditions: 1.2 mM NADH, 15 units/mL LDH, 100 mM HEPES pH 7.5, 20 mM MgCl_2 , $T = 25 \text{ }^\circ\text{C}$. Measurements without and with 1.2 mM pyruvate were carried out. The bias voltage U_{bias} was varied. The resulting amplitudes of the photocurrent versus the bias voltage are displayed in Figure SI-II.1.4.

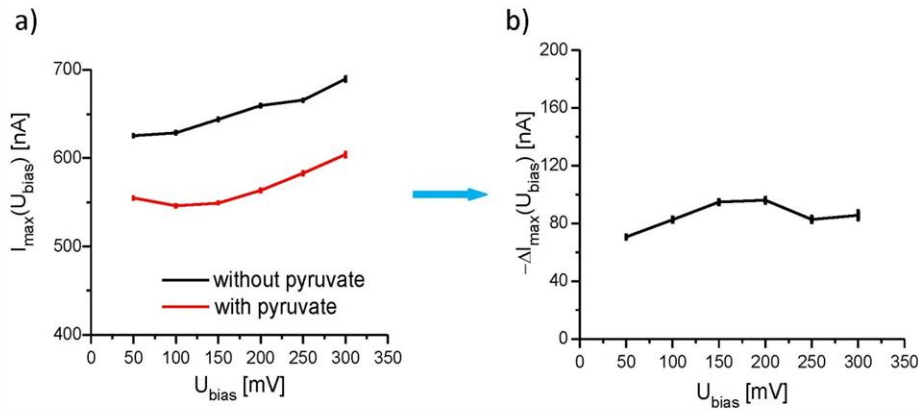


Figure SI-II.1.4: a) Amplitude of the photocurrent I_{\max} versus the applied bias U_{bias} , as derived from the data shown in Figure SI-II.1.3. The reaction according to Eq. 3 was carried out using the following conditions: 1.2 mM NADH, 15 units/mL LDH, 100 mM HEPES pH 7.5, 100 mM KCl, 20 mM MgCl_2 , $T = 25^\circ\text{C}$. Measurements without and with 1.2 mM pyruvate were performed. The bias voltage U_{bias} was varied. b) The difference in photocurrent amplitude with and without pyruvate is plotted: $\Delta I_{\max}(U_{\text{bias}}) = I_{\max}^{\text{w pyruvate}}(U_{\text{bias}}) - I_{\max}^{\text{wo pyruvate}}(U_{\text{bias}})$.

II.2) Photocurrent measurements of the QD electrode with the reactants of the first enzyme reaction

The guanylate kinase reaction is sketched in Figure SI-II.2.1. Photocurrent measurements $I(t)$ in the presence of ATP, with and without GMPK, and variable GMP concentration are shown in Figure SI-II.2.2. The concentration dependence is shown in Figure SI-II.2.3. Enzymes (here GMPK) were free in solution.

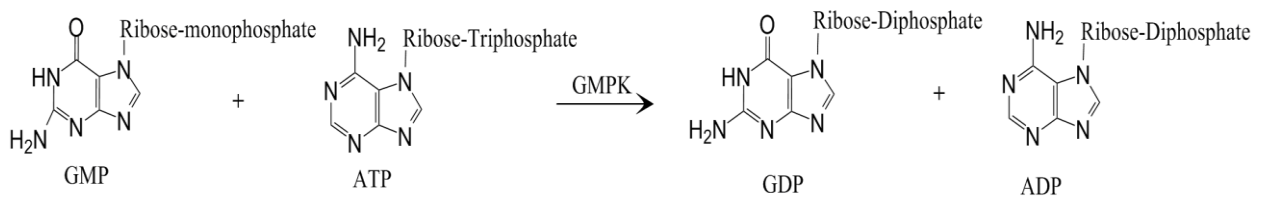


Figure SI-II.2.1: Schematic of the 1st reaction representing phosphoryl group transfer from ATP to GMP catalyzed by the enzyme guanylate kinase.

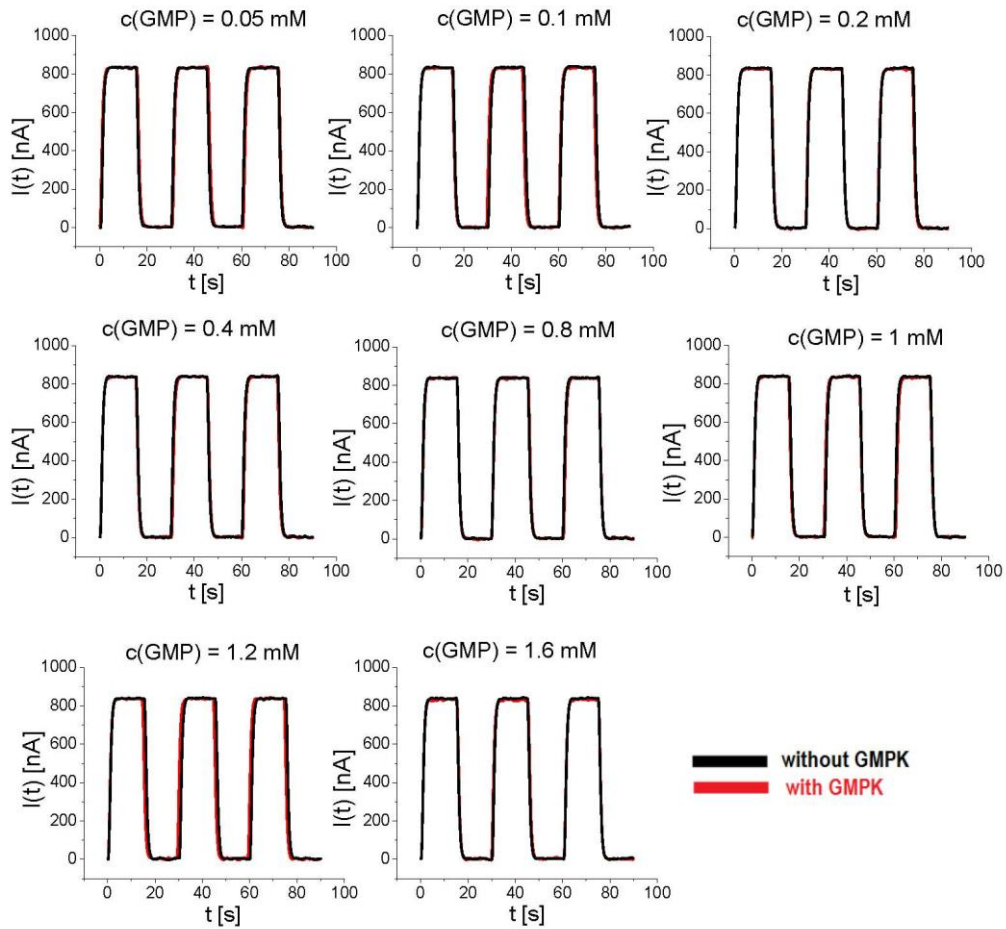


Figure SI-II.2.2: Photocurrent measurements $I(t)$ following the reaction of Eq. 1 with the following conditions: 4 mM ATP, 100 mM HEPES, pH 7.5, 100 mM KCl, 20 mM $MgCl_2$, $U_{bias} = +50$ mV, $T = 25$ °C. GMPK was optionally added at 18 nM. The GMP concentrations were varied from 0.05 mM to 1.6 mM. The resulting amplitudes of the photocurrent versus the GMP concentration $I_{max}(c(GMP))$ are displayed in Figure SI-II.2.3.

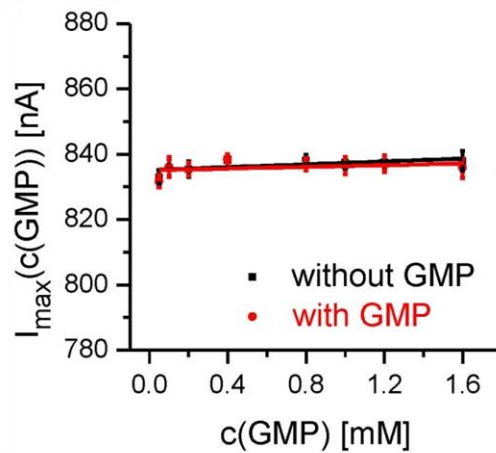


Figure SI-II.2.3: Amplitude of the photocurrent I_{max} versus GMP concentration, as derived from the data shown in Figure SI-II.2.2.

II.3) Photocurrent measurements of the QD electrode in solutions with the reactants of the first and second enzyme reaction

The pyruvate kinase reaction is sketched in Figure SI-II.3.1. Photocurrent measurements $I(t)$ in the presence of ATP, with and without GMPK, and variable GMP concentration are shown in Figure SI-II.3.2, *i.e.* reactions combining steps 1 and 2. The concentration dependence is shown in Figure SI-II.3.3. Enzymes (here PK and GMPK) were free in solution.

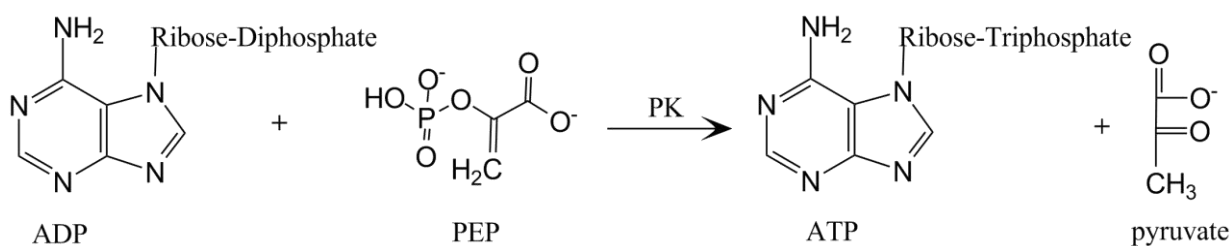


Figure SI-II.3.1: Schematic of the 2nd reaction catalyzed by pyruvate kinase.

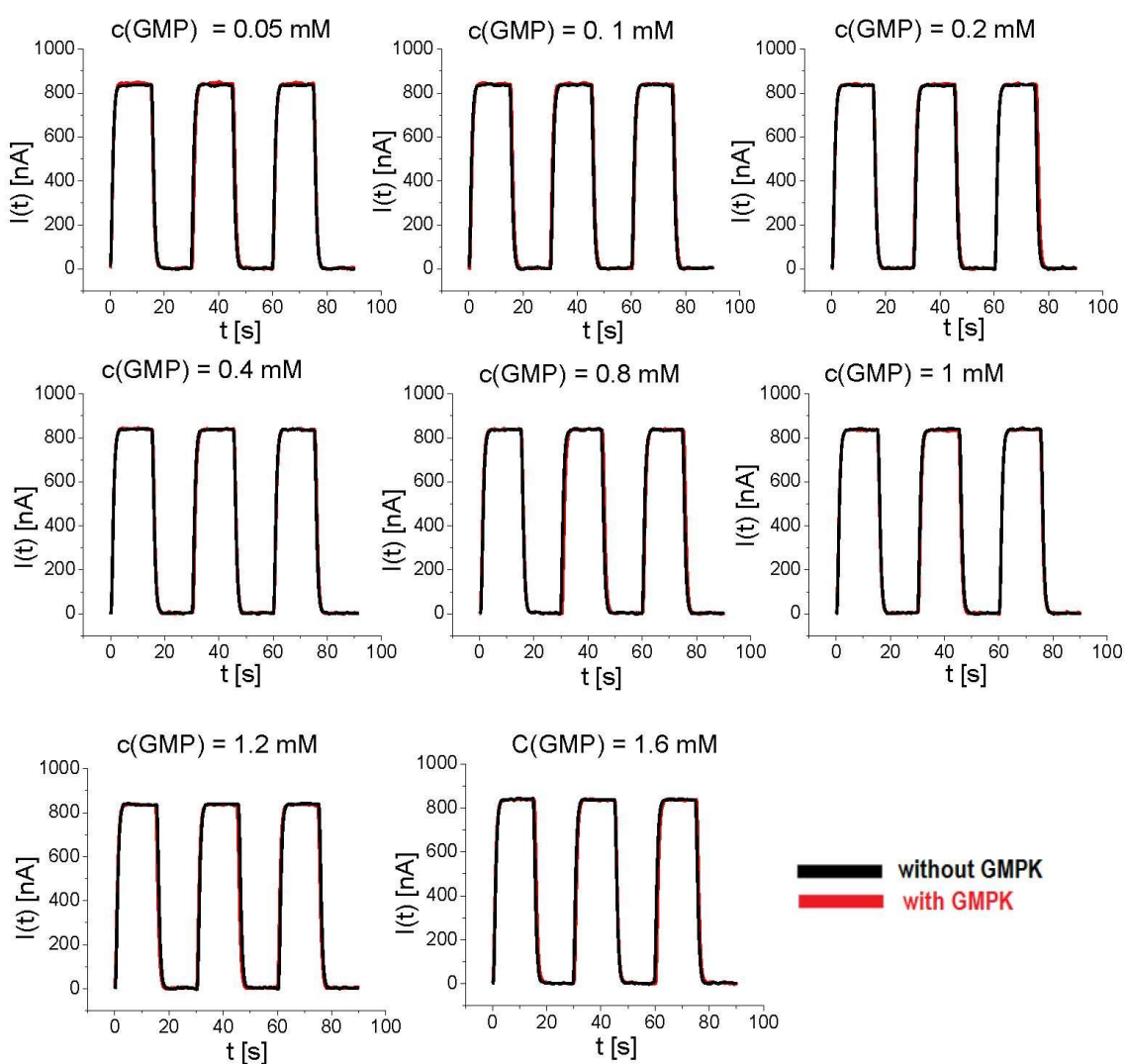


Figure SI-II.3.2: Photocurrent measurements $I(t)$ following the combined reactions of Eq. 1 and Eq. 2 with the following conditions: 4 mM ATP, 2 mM PEP, 12 units/mL PK, 100 mM

HEPES, pH 7.5, 100 mM KCl, 20 mM MgCl₂, $U_{bias} = +50$ mV, $T = 25$ °C. GMPK was optionally added at 18 nM. The GMP concentrations were varied from 0.05 mM to 1.6 mM. The resulting amplitudes of the photocurrent versus the GMP concentration $I_{max}(c(GMP))$ are displayed in Figure SI-II.3.3.

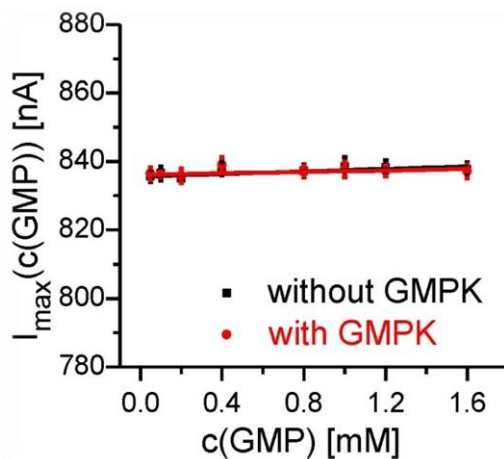


Figure SI-II.3.3: Amplitude of the photocurrent I_{max} versus GMP concentration, as derived from the data shown in Figure SI-II.3.2.

II.4) Photocurrent measurements of the QD electrode with all the three enzymes in solution

In this paragraph, results for the combination of all three reactions according to equations 1-3 are shown. Enzymes (*i.e.* PK, LDH, and GMPK) were free in solution. Photocurrent measurements $I(t)$ in the presence of ATP, PEP, NADH, PK, LDH, with and without GMPK, and variable GMP concentration are shown in Figure SI-II.4.1. The concentration dependence is shown in Figure 4 of the main text.

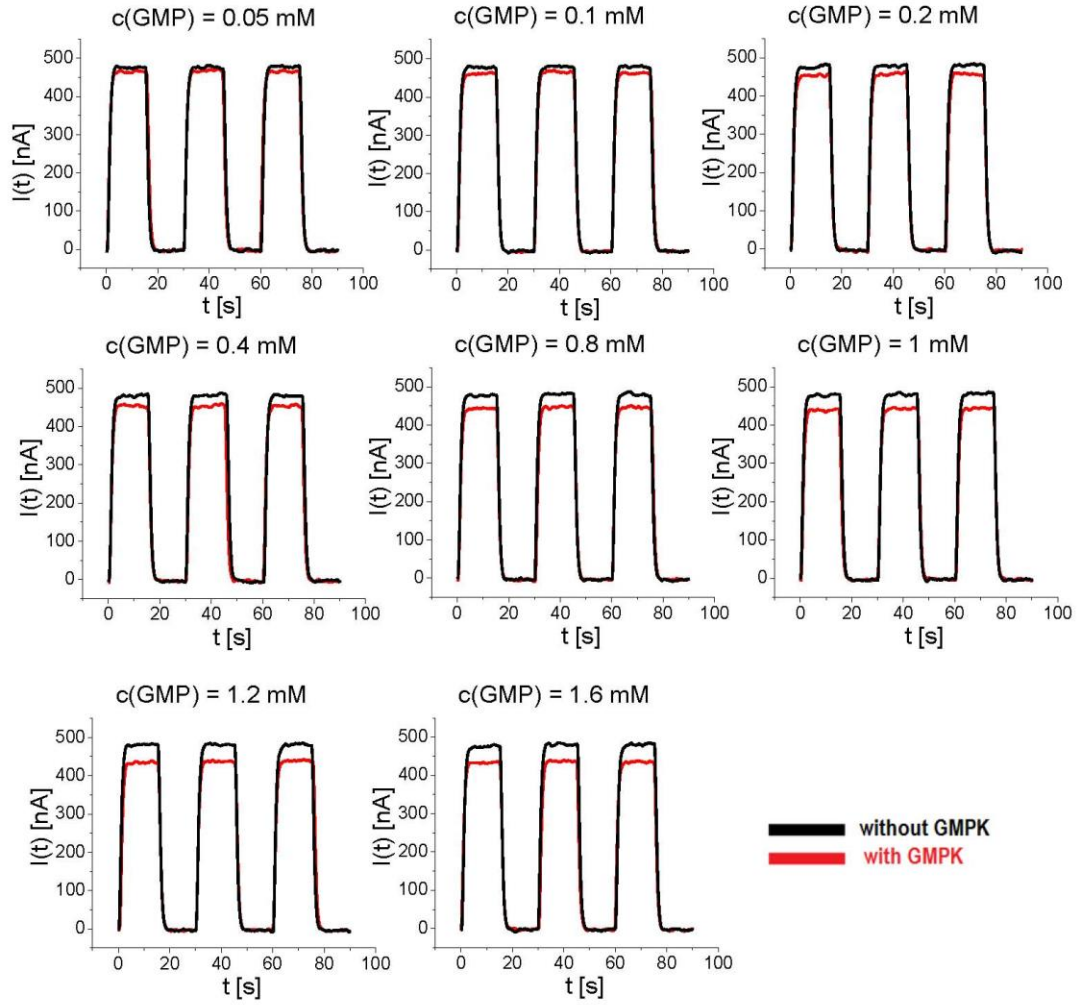


Figure SI-II.4.1: Photocurrent measurements $I(t)$ following the combined reactions of Eq. 1, Eq. 2, and Eq. 3 with the following conditions: : 1.2 mM NADH, 4 mM ATP, 2 mM PEP, 12 units/mL PK, 15 units/mL LDH, 100 mM HEPES, pH 7.5, 100 mM KCl, 20 mM $MgCl_2$, $U_{bias} = +50$ mV, $T = 25$ °C. GMPK was optionally added at 18 nM. The GMP concentrations were varied from 0.05 mM to 1.6 mM. The resulting amplitudes of the photocurrent versus the GMP concentration $I_{max}(c(GMP))$ are displayed in Figure 3 of the main text.

II.5) Photocurrent measurements of the QD sensor electrode immobilized enzymes

In this paragraph, results for the combination of all three reactions according to equations 1-3 are shown. Here, LDH, PK and GMPK were immobilized on the QD-modified electrode. Photocurrent measurements $I(t)$ in the presence of ATP, PEP, NADH, LDH, PK, GMPK and with/ without variable GMP concentration are shown in Figure SI-II.5.1. The concentration dependence is shown in Figure 5 of the main text.

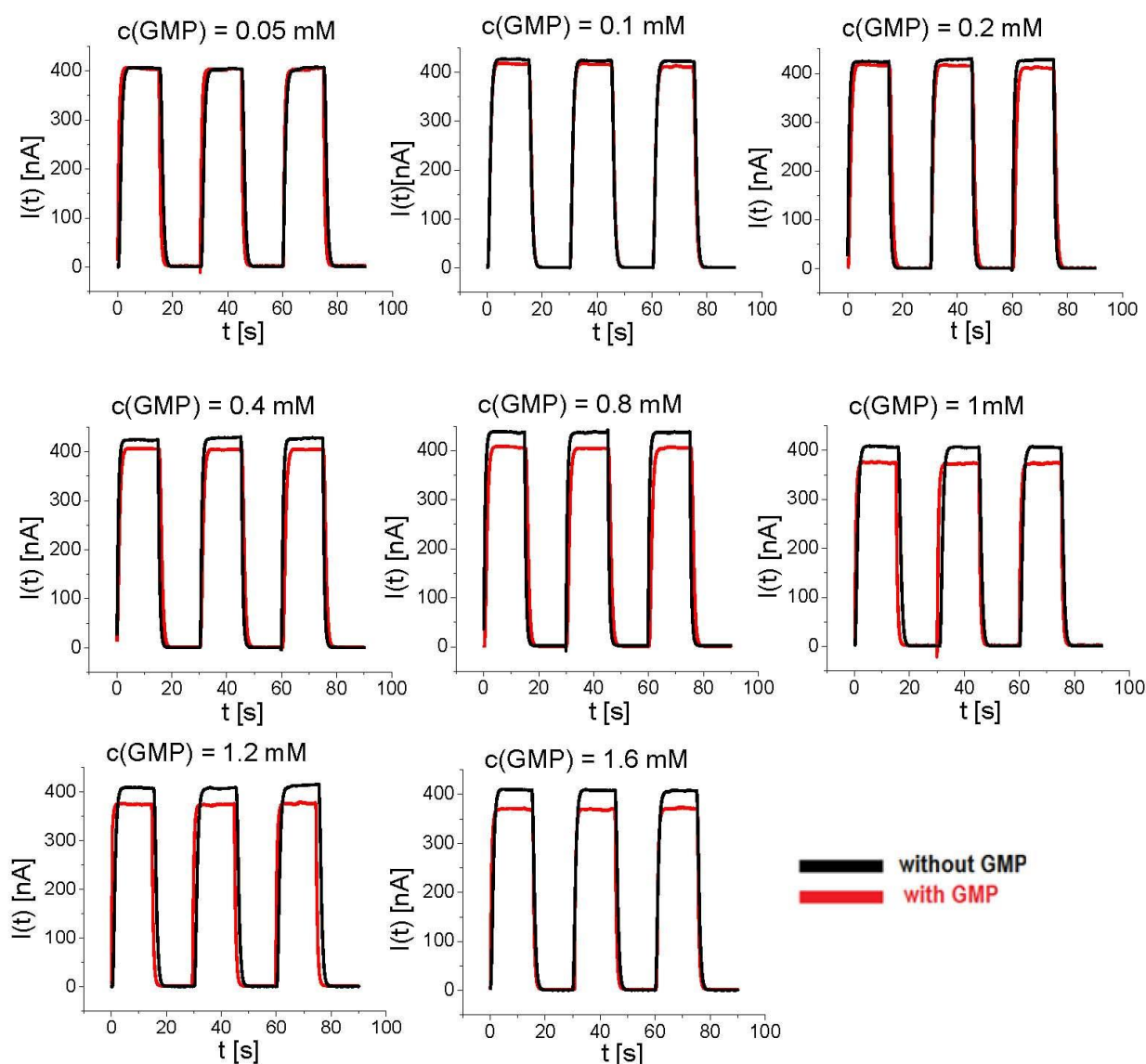


Figure SI-II.5.1: Photocurrent measurements $I(t)$ following the combined reactions of Eq. 1, Eq. 2, and Eq. 3 with the following conditions: 1.2 mM NADH, 4 mM ATP, 2 mM PEP, 100 mM HEPES, pH 7.5, 100 mM KCl, 20 mM MgCl₂, $U_{bias} = +50$ mV, $T = 25$ °C. Here, 6 μ L of 18 nM GMPK, 12 units PK and 15 units LDH were immobilized on the QDs layer. The GMP concentrations were varied from 0.05 mM to 1.6 mM. The resulting amplitudes of the photocurrent versus the GMP concentration $I_{max}(c(GMP))$ are displayed in Figure 5 of the main text.

As in all coupled enzymatic test systems the presence of intermediates such as ADP or GDP in the conversion cycle would change the response of the read-out of the coupled three reactions. However the three-step coupled-enzyme assay as presented in this work has the advantage of being a modular setup allowing for independent detection of each reaction. Therefore, in the absence of guanylate kinase, the pyruvate kinase-catalyzed reaction can be monitored to first detect the presence of ADP and/or GDP, thus excluding interference with the detection of GMP, and this applies even to cellular extracts.

III) References

- [1] N. Sekulic, L. Shuvalova, O. Spangenberg, M. Konrad, A. Lavie, *J. Biol. Chem.* **2002**, 277 (33), 30236-30243.
- [2] W. W. Yu, X. Peng, *Angew. Chem. Int. Ed.* **2002**, 41 (13), 2368-2371.
- [3] H. Y. Chen, S. Maiti, D. H. Son, *ACS Nano* **2012**, 6 (1), 583-591.
- [4] C.-A. J. Lin, R. A. Sperling, J. K. Li, T.-Y. Yang, P.-Y. Li, M. Zanella, W. H. Chang, W. J. Parak, *Small* **2008**, 4 (3), 334-341.
- [5] W. W. Yu, L. Qu, W. Guo, X. Peng, *Chem. Mater.* **2003**, 15 (14), 2854-2860.
- [6] B. O. Dabbousi, J. Rodriguez-Viejo, F. V. Mikulec, J. R. Heine, H. Mattoussi, R. Ober, K. F. Jensen, M. G. Bawendi, *J. Phys. Chem. B* **1997**, 101 (46), 9463-9475.
- [7] W. Khalid, M. E. Helou, T. Murböck, Z. Yue, J.-M. Montenegro, K. Schubert, G. Göbel, F. Lisdat, G. Witte, W. J. Parak, *ACS Nano* **2011**, 5 (12), 9870-9876.
- [8] W. Khalid, G. Göbel, D. Hühn, J.-M. Montenegro, P. Rivera Gil, F. Lisdat, W. J. Parak, *J. Nanobiotechnol.* **2011**, 9, 46.
- [9] Z. Yue, W. Khalid, M. Zanella, A. Z. Abbasi, A. Pfreundt, P. Rivera_Gil, K. Schubert, F. Lisdat, W. J. Parak, *Anal. Bioanal. Chem.* **2010**, 396 (3), 1095-1103.